Effects of thermal treatment on the formation of the columnar structures in ZnO thin films grown on p-Si (100) substrates

Cite as: J. Appl. Phys. **100**, 013526 (2006); https://doi.org/10.1063/1.2214366
Submitted: 21 February 2006 • Accepted: 19 April 2006 • Published Online: 13 July 2006

J. W. Shin, J. Y. Lee, Y. S. No, et al.

Effects of thermal treatment on the formation of the columnar structures in ZnO thin films grown on *p*-Si (100) substrates

J. W. Shin and J. Y. Lee
Department of Materials Science and Engineering, Korea Advanced Institute of Science and Technology, Daejeon 305-701, Korea

Y. S. No and T. W. Kim[a)]
Division of Electronics and Computer Engineering, Hanyang University, Seoul 133-791, Korea

W. K. Choi
Thin Film Material Research Center, Korea Institute of Science and Technology, Seoul 136-701, Korea

(Received 21 February 2006; accepted 19 April 2006; published online 13 July 2006)

X-ray diffraction patterns showed that crystallinity of the annealed ZnO films was improved by thermal annealing. Transmission electron microscopy images showed that columnar structures were preferentially formed in ZnO thin films due to thermal annealing, and electron energy loss spectroscopy images showed that annealing caused O_2 atoms to diffuse out from the upper region in the ZnO thin film. The effects of thermal treatment on the formation of the columnar structures in ZnO thin films grown on Si (100) substrates are described on the basis of the experimental results. © *2006 American Institute of Physics*. [DOI: 10.1063/1.2214366]

I. INTRODUCTION

ZnO semiconductors have emerged as excellent candidates for possible applications in the fabrication of optoelectronic devices operating in the blue region of the spectrum.[1–5] Since ZnO thin films have physical properties such as large exciton binding energies and excellent chemical stabilities,[6,7] they have drawn a great deal of interest because of the feasibility of applications in next-generation optoelectronic devices, such as light-emitting diodes,[8] laser diodes,[9] and solar cells.[10] ZnO/Si heterostructures have the hybrid advantages of the large exciton binding energy of the ZnO thin film and the cheapness and the large size of the Si substrate.[11] Even though some works concerning ZnO/Si heterostructures have been reported,[12,13] few works on the effects of thermal treatment on the formation of the columnar structures in ZnO thin films grown on *p*-Si (100) substrates have been performed. Since the optical properties of ZnO thin films are strongly affected by their microstructural properties, studies concerning the effects of annealing on the microstructural properties of ZnO thin films and ZnO/Si heterostructures are necessary for fabricating high-quality optoelectronic devices utilizing ZnO/Si heterostructures. Even though some works concerning the microstructure and the crystal defects in ZnO epitaxial films grown on (0001) sapphire substrates have been reported,[14,15] systematic studies concerning the effect of thermal treatment on the formation of the columnar structures in ZnO thin films grown on Si substrates may play a very important role in enhancing device efficiency.

This paper reports data on the effects of thermal treatment on the formation of the columnar structures in ZnO thin films grown on *p*-Si (100) substrates by using radio-frequency magnetron sputtering. X-ray diffraction (XRD) measurements were carried out to investigate the crystallization of the ZnO thin films. Transmission electron microscopy (TEM) measurements was carried out in order to investigate the microstructural properties of the ZnO/*p*-Si (100) heterostructures, and electron energy loss spectroscopy (EELS) measurements were performed to investigate the distribution of the oxygen in the ZnO thin films. The formation of the columnar structures of the ZnO thin films grown on Si (100) substrates are described on the basis of the experimental results.

II. EXPERIMENTAL DETAILS

Polycrystalline stoichiometric ZnO with a purity of 99.999% was used as a source target material and was precleaned by repeated sublimation. The carrier concentration of the B-doped *p*-Si substrates with (100) orientations used in this experiment was 1×10^{15} cm^{-3}. The substrates were degreased in trichloroethylene (TCE), rinsed in de-ionized water, etched in a mixture of HF and H_2O (1:1) at room temperature for 5 min, and rinsed in TCE again. After the Si wafers had been cleaned chemically, they were mounted onto a susceptor in a growth chamber. After the chamber had been evacuated to 8×10^{-7} Torr, the deposition was done at a substrate temperature of 600 °C. Ar gas with a purity of 99.999% was used as the sputtering gas. Prior to ZnO growth, the surface of the ZnO target was polished by Ar^+ sputtering. The ZnO deposition was done at a system pressure of 0.021 Torr and a radio-frequency power (radio frequency=13.26 MHz) of 100 W. The flow-rate ratio of Ar to O_2 was 2, and the growth rate was approximately 1.17 nm/min. The thermal annealing process was performed in a nitrogen atmosphere with a tungsten-halogen lamp as the thermal source. The thermal annealing process was carried out for 5 min at 900 °C.

[a)]Author to whom correspondence should be addressed; electronic mail: twk@hanyang.ac.kr

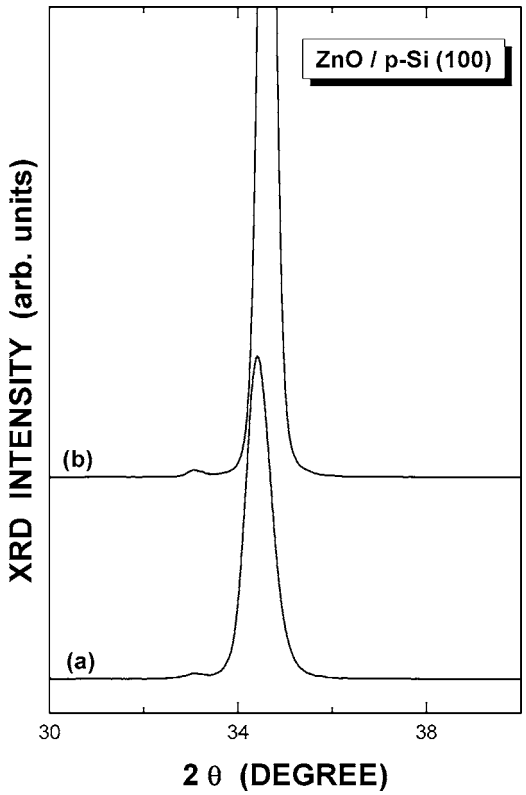

FIG. 1. X-ray diffraction patterns of the (a) as-grown and the (b) annealed ZnO thin films grown on *p*-Si (100) substrates.

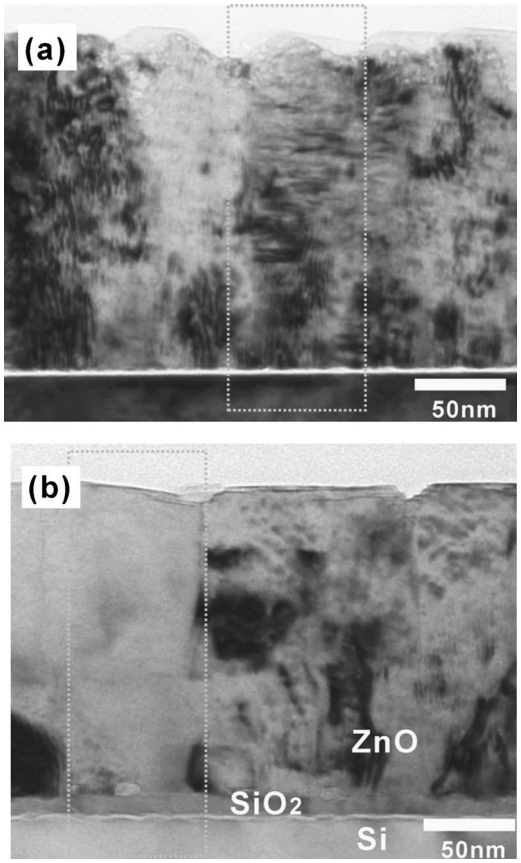

FIG. 2. Cross-sectional bright-field transmission electron microscopy images of the (a) as-grown and the (b) annealed ZnO thin films grown on *p*-Si (100) substrates.

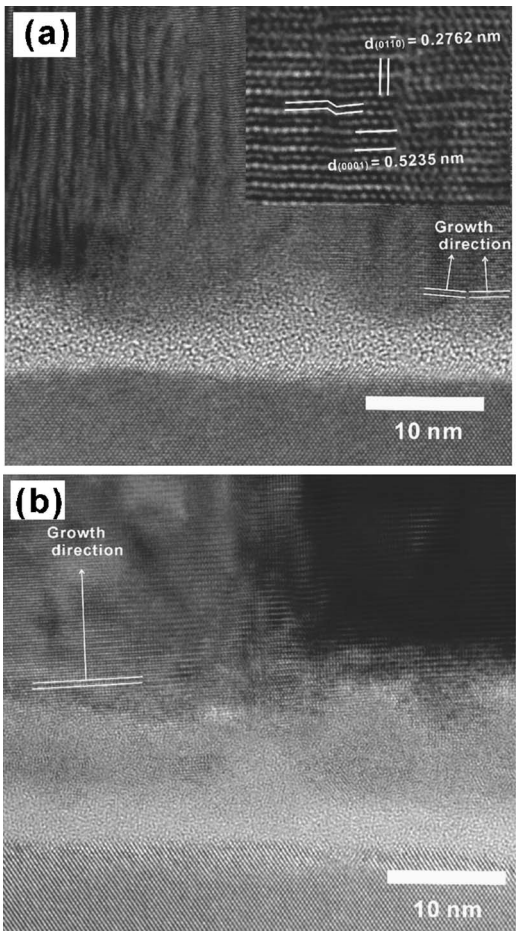

FIG. 3. High-resolution transmission electron microscopy images of the (a) as-grown and the (b) annealed ZnO thin films with interfacial layers grown on *p*-Si (100) substrates.

The XRD measurements were performed by using a Rigaku D/Max-B diffractometer with Cu $K\alpha$ radiation. The TEM measurements were performed using a JEM-ARM 1300S transmission electron microscope operating at 1.25 MeV. The samples for the cross-sectional TEM measurements were prepared by cutting and polishing with diamond paper to a thickness of approximately 30 μm and then argon-ion milling at liquid-nitrogen temperature to electron transparency. The EELS measurements for oxygen mapping were performed by using a HV-GIF EELS system.

III. RESULTS AND DISCUSSION

The XRD patterns in Fig. 1 for the (a) as-grown and the (b) annealed ZnO films grown on *p*-Si (100) substrates clearly show (0002) $K\alpha_1$ diffraction peaks at 34.41° and 34.60° for the as-grown and the annealed ZnO (0001) films, respectively. The *c* values of the as-grown and the annealed ZnO thin films, as determined from the Bragg equation, are 0.5213 and 0.5185 nm, respectively. While the *c* value of the as-grown ZnO thin film is larger than that of the ZnO bulk (0.5204 nm), that of the annealed ZnO thin film is smaller. This behavior was observed in previous works.[16–18] The XRD patterns for the as-grown and the annealed ZnO thin films grown on Si (100) substrates indicate that the as-grown and the annealed ZnO films have a strong *c*-axis orientation,

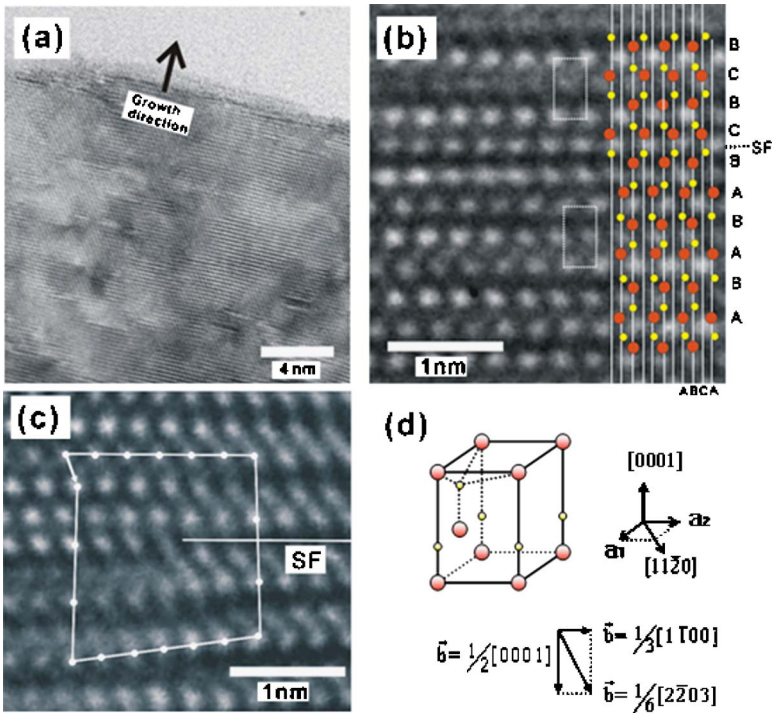

FIG. 4. (a) High-resolution transmission electron microscopy of the upper region for the annealed ZnO thin films showing a high density of stacking faults. (b) High-resolution image of the intrinsic-type stacking faults. (c) High-resolution TEM image of a partial dislocation of the ZnO thin film with a Burgers vector $b = 1/6[02\bar{2}3]$ around a stacking fault. (d) Schematic diagram of the ZnO thin film; the smaller and the larger circles denote Zn and O, respectively.

that orientation giving the lowest surface free energy. The intensity of the XRD pattern related to the ZnO (0001) film for the annealed ZnO/Si heterostructure is larger than that for the as-grown samples, and the full width at half maximum for the (0002) ZnO diffraction peak for the annealed ZnO/Si heterostructure is smaller than that for the as-grown sample, indicative of a more preferential orientation of the (0001) hexagonal structure after thermal annealing.

Figure 2 shows cross-sectional bright-field TEM images of the (a) as-grown and the (b) annealed ZnO thin films grown on *p*-Si (100) substrates. The top side of the ZnO thin film, the bottom side of the Si substrate, and the SiO_2 interfacial layer are shown in Fig. 2. High-resolution TEM (HRTEM) images of the (a) as-grown and the (b) annealed ZnO thin films grown on *p*-Si (100) substrates are shown in Fig. 3. The interplanar spacing distance of the $(0001)_{ZnO}$ of the as-grown ZnO film is 0.5235 nm, and the as-grown ZnO thin film receives a tensile stress along the *c* axis, which is in reasonable agreement with the XRD result. Since the interplanar spacing distance of the $(01\bar{1}0)_{ZnO}$ direction for the as-grown ZnO film is 0.2762 nm, the as-grown ZnO thin film receives a compressive strain along the *a* axis. The bottom side of the as-grown ZnO film is significantly distorted, and many stacking faults are observed in the as-grown ZnO

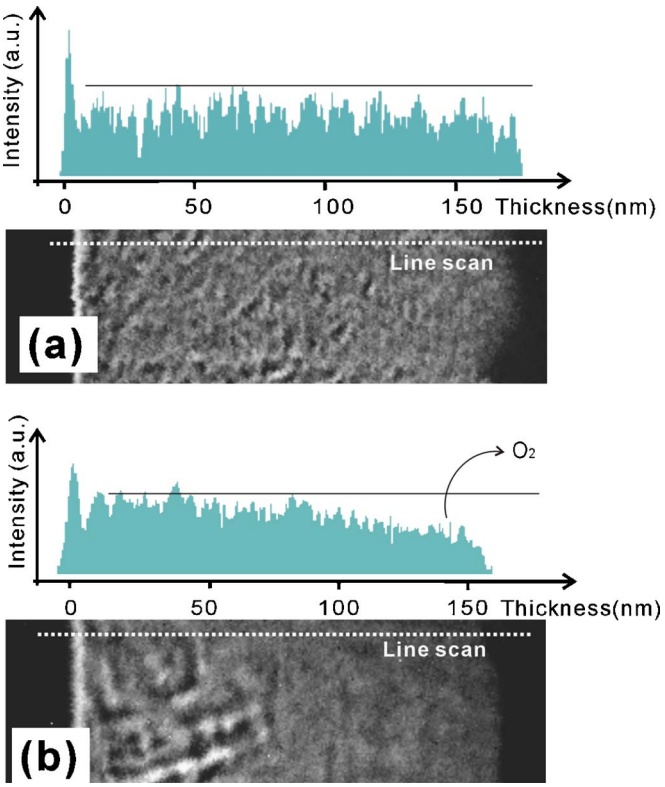

FIG. 5. Electron energy loss spectroscopy maps obtained from the square area in Fig. 2. The histogram obtained from the line scan indicates the distribution of oxygen in the ZnO film.

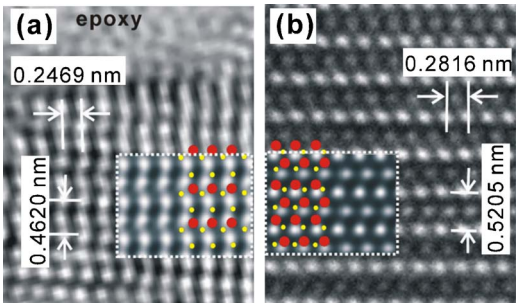

FIG. 6. High-resolution transmission electron microscopy images obtained at the (a) top region and the (b) lower region for the annealed ZnO thin film. The insets show both the tentative model of the oxygen vacancy in the ZnO thin film and a simulated image, obtained from the NCMSS software, of a ZnO thin film with perfect stoichiometry. The smaller and the larger circles denote Zn and O atoms, respectively.

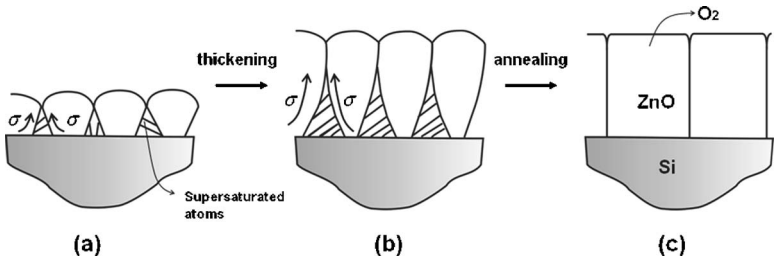

FIG. 7. Schematic diagrams for the effects of thermal annealing on the formation of columnar structures in ZnO thin films grown on *p*-Si (100) substrates due to thermal annealing.

film due to the supersaturated population of the adatoms during the nucleation and the coalescence of the molecules.[19] The upper region of the ZnO columnar structure is more stable than its lower region, as shown in Fig. 2. After coalescence, the ZnO columnar structure in the lower region consists of grains in a nonequilibrium state.[19] Because the shape of a grain island is convex and because the upper region of the ZnO columnar structure is closer to an equilibrium state due to atomic mobility during deposition, stress relaxation is more fully achieved in the upper region than in the lower region. This result suggests that the lower angle shift of the XRD peak for the as-grown ZnO thin film, in comparison with that of the bulk ZnO, originates from an intrinsic property rather than from a thermal effect during deposition.

The structure of the bottom region in the annealed ZnO thin film is shown in Fig. 3(b) and indicates that the stress in the lower region of the ZnO thin film was relaxed during annealing, which affects the atomic mobility. The number of stacking faults in the upper region is more than that in the lower region, as shown in Fig. 4(a). These intrinsic-type stacking faults, which are characterized by a stacking sequence *ABAB*/*CBCB*, as shown in Fig. 4(b), have partial dislocations with the Burgers vector $b=1/6[02\bar{2}3]$ around a stacking fault, as shown in Fig. 4(c). This behavior is in reasonable agreement with the results reported by Sun *et al.*[15] Stacking faults are generated due to concentrations of vacancies or interstitials, which leads to a missing or additional (0002) plane.[14] Since thermal treatment of ZnO thin films tends to cause oxygen atoms to diffuse out from the ZnO layer,[20] the stacking faults observed in the annealed ZnO thin film are due to concentration of oxygen vacancies, which is in reasonable agreement with the XRD results; the $K\alpha_1$ diffraction peak for the annealed ZnO thin films shifts to higher angle in comparison with that for the ZnO bulk, indicative of a decrease in the interplanar spacing distance, which can be attributed to the formation of the oxygen vacancies. Even though oxygen atoms exist in the crystal in the forms of O^{2-} ions, they become neutral O atoms, resulting in the formation of the O_2 gas.[20] The decrease in the number of oxygen atoms in the upper region is confirmed from the histogram obtained from the line scan in the EELS map, which is shown in Fig. 5. Since the number of oxygen atoms in the ZnO thin film significantly decreases with increasing film thickness, while the stacking faults appear around the middle region in the ZnO film, the oxygen vacancy layers are formed at the top region due to the dramatic decrease in the number of oxygen atoms.

The HRTEM images obtained at the (a) top region and the (b) lower region for the annealed ZnO thin film are shown in Fig. 6. The inserts show the tentative models and the simulated results, which correspond to the HRTEM images obtained at the top and lower regions for the annealed ZnO thin film and were constructed by using the NCMSS software, for ZnO films with an oxygen vacancy layer and with perfect stoichiometry. The atomic spacing distances in the $(0001)_{ZnO}$ and the $(01\bar{1}0)_{ZnO}$ planes of the lower region of the ZnO film are 0.5205 and 0.2815 nm, respectively, which are almost the same as those of the ZnO bulk. However, the atomic spacing distances in the $(0001)_{ZnO}$ and the $(01\bar{1}0)_{ZnO}$ planes of the top region of the ZnO film are 0.4620 and 0.2469 nm, respectively. The atomic spacing distance significantly decreases due to formation of an oxygen vacancy layer at the top of the ZnO thin film.

The formation of the columnar structures in the annealed ZnO with *c* axis film is shown in Fig. 7. Since the nucleation frequencies in deposition processes are so high that the nuclear spacings are very small,[21] the columnar structures consist of nonequilibrium states due to the supersaturated population of adatoms during the nucleation and the coalescence of the molecules, as shown in Fig. 7(a). Since stress relaxation is more fully achieved in the upper region than in the lower region during deposition, the upper region of the ZnO columnar structure is more stable than the lower region in as-grown ZnO thin films, as shown in Fig. 7(b). After thermal annealing, the intrinsic stress in as-grown ZnO thin films can be accommodated. However, a stoichiometry problem is generated in the upper region due to oxygen vacancies, as shown in Fig. 7(c).

IV. SUMMARY AND CONCLUSION

The results of XRD, TEM, and selected area diffraction pattern (SADP) measurements showed that columnar structures with *c* axis were preferentially formed in the ZnO thin films due to thermal annealing. EELS maps showed that oxygen atoms diffused out of the ZnO thin film during thermal treatment, which indicates that additional effects of annealing must be considered. The formation of the columnar structures with the *c*-axis preferential orientations in ZnO thin films grown on Si (100) substrates was described.

ACKNOWLEDGMENTS

This work was supported by the Korea Science and Engineering Foundation through the Quantum-Functional Semiconductor Research Center at Dongguk University and by a grant (code No. 05K1501-02510) from the Center for Nanostructured Materials Technology under 21st Century

Frontier R&D Programs of the Ministry of Science and Technology, Korea. The authors would like to thank Dr. Youn-Joong Kim at the Korea Basic Science Institute for the use of the HVEM.

[1]R. F. Service, Science **276**, 895 (1997).
[2]D. M. Bagnall, Y. F. Chen, Z. Zhu, T. Yao, M. Y. Shen, and T. Goto, Appl. Phys. Lett. **73**, 1038 (1998).
[3]A. Nahhas, H. K. Kim, and J. Blachere, Appl. Phys. Lett. **78**, 1511 (2001).
[4]V. A. Fonoberov and A. A. Balandin, Appl. Phys. Lett. **85**, 5971 (2004).
[5]W. Shen, W. Walukiewicz, J. W. Ager III, K. M. Yu, H. B. Yuan, H. P. Xin, G. Cantwell, and J. J. Song, Appl. Phys. Lett. **86**, 191911 (2005).
[6]T. Soki, Y. Hatanaka, and D. C. Look, Appl. Phys. Lett. **76**, 3257 (2000).
[7]S. Hong, T. Joo, W. I. Park, Y. H. Jun, and G.-C. Yi, Appl. Phys. Lett. **83**, 4157 (2003).
[8]Y. Liu, C. R. Gorla, S. Liang, N. Emanetoglu, Y. Lu, H. Shen, and M. Wraback, J. Electron. Mater. **29**, 60 (2000).
[9]H. Kim *et al.*, Appl. Phys. Lett. **76**, 259 (2000).
[10]U. Rau and M. Schmidt, Thin Solid Films **387**, 141 (2001).
[11]A. Nahhas, H. K. Kim, and J. Blachere, Appl. Phys. Lett. **78**, 1511 (2001).
[12]B. Guo, Z. R. Qiu, and K. S. Wong, Appl. Phys. Lett. **82**, 2290 (2003).
[13]S. H. Jeong, B. S. Kim, and B. T. Lee, Appl. Phys. Lett. **82**, 2625 (2003).
[14]D. Gerthsen, D. Litvinov, Th. Gruber, C. Kirchner, and A. Wang, Appl. Phys. Lett. **81**, 3972 (2002).
[15]H. P. Sun, X. Q. Pan, X. L. Du, Z. X. Mei, Z. Q. Zeng, and Q. K. Xue, Appl. Phys. Lett. **85**, 4385 (2004).
[16]R. Hong, J. Huang, H. He, Z. Fan, and J. Shao, Appl. Surf. Sci. **242**, 346 (2005).
[17]G. Du *et al.*, Vacuum **69**, 473 (2003).
[18]V. Gupta and A. Mansingh, J. Appl. Phys. **80**, 1063 (1998).
[19]C. V. Thompson, Annu. Rev. Mater. Sci. **30**, 159 (2000).
[20]R. A. Swalin, *Thermodynamics of Solids* (Wiley, Toronto, Canada, 1972), pp. 335–341.
[21]C. V. Thompson and R. Carel, Mater. Sci. Eng., B **32**, 211 (1995).